Modelling of bond behaviour by means of sequentially linear analysis and concrete-to-steel interface elements

Ensink, Sebastiaan; van de Graaf, Anne; Slobbe, A.T.; Hendriks, Max; den Uijl, Joop; Rots, Jan

Publication date
2012

Published in
Proceedings of the Fourth International Symposium" Bond in concrete 2012: Bond, Anchorage, Detailing"

Citation (APA)
Ensink, S., van de Graaf, A., Slobbe, A. T., Hendriks, M., den Uijl, J., & Rots, J. (2012). Modelling of bond behaviour by means of sequentially linear analysis and concrete-to-steel interface elements. In J. Cairns, G. Metelli, & G. A. Plizzari (Eds.), *Proceedings of the Fourth International Symposium" Bond in concrete 2012: Bond, Anchorage, Detailing": General aspects of bond* (Vol. 1, pp. 161-167).

Modelling of bond behaviour by means of sequentially linear analysis and concrete-to-steel interface elements

S.W.H. Ensink, A.V. van de Graaf, A.T. Slobbe, M.A.N. Hendriks, J.A. den Uijl, J.G. Rots
Delft University of Technology, P.O. Box 5048, 2600 GA Delft, the Netherlands

ABSTRACT: In the present paper a sequentially linear approach is proposed to model bond-slip using interface elements. Within a finite element framework this requires piecewise constant material behaviour: saw-tooth approximations. Using a similar approach as with concrete softening, a generic saw-tooth approximation is presented for bond-slip. In conjunction with a concrete cracking model and steel plasticity the new bond-slip model will be incorporated to investigate the possibility to model a tension-pull experiment. The use of axisymmetric elements within a sequentially linear analysis framework will be introduced to model a circular concrete cross-section. A straightforward tension-pull experiment will serve as a base for comparison between conventional nonlinear finite element analysis and sequential linear analysis. This will validate the sequentially linear approach for both bond-slip interface elements as well as for axisymmetric elements. The next step is to analyse a tension-pull experiment without the use of material imperfections. Material imperfections are normally necessary in a conventional nonlinear analysis in order to trigger crack localizations. Finally using an adapted bond model by Bigaj to compute the bond-slip curve, variations in the material parameters such as the amount of reinforcement and concrete quality are explored, resulting in characteristic crack spacings.

1 INTRODUCTION

In nonlinear finite element analysis (NLFEA) of concrete fracture, computational problems can arise such as non-convergence or bifurcations due to sharp material "softening" after realization of the material strength. These types of problems become of more importance when dealing with a structure that initially has a nearly uniform stress distribution, for example in a tension-pull experiment. Often the nonlinear analysis is impeded by simultaneous cracking in a large part of the structure. This makes it practically difficult to incorporate bond-slip models which are essential for a true simulation of crack patterns.

For brittle materials an attractive alternative method to NLFEA is Sequentially Linear Analysis or SLA for short. With SLA the analysis consists of increments of damage instead of an increment of displacement, force, arc-length or time (Rots et al. 2008). The SLA approach can be referred to as an "event-by-event" procedure. In each step a critical integration point (i.p.) is identified for which the ratio between the stress level and its current strength is the highest in the whole structure. The critical i.p. will provide a 'global load factor'. The present solution step is obtained by rescaling the 'unit load elastic solution' times the 'global load factor'. The critical i.p. will then be reduced in strength and stiffness, according to a saw-tooth constitutive law (see Section 3). This corresponds to a local damage "event". These steps will then be repeated until the damage has spread into the structure to the desired level. In this way damage that occurs in a structure can be covered in detail from start to finish and none of the structural response is lost during the analysis. This makes it well suited for the analysis of a tension-pull experiment where the stress state is inherently uniform.

In this paper the focus is to model bond-slip in conjunction with SLA with the use of concrete-to-steel interface elements. The outlook is that such a modelling approach would facilitate robust finite element analysis on structural level, with accurate bond-slip modelling on local level. The results will be compared to experimental and conventional nonlinear analysis results.

For the interface elements a bond stress-slip relation is calculated using an adapted bond model by Bigaj (1999). This model takes into account both material and structural properties such as the amount of concrete cover which makes it well suited to investigate various variations of tension-pull experiments. The bond model is made suitable for application in SLA by means of saw-tooth curve generation. For the modelling of the circular concrete cross-section axisymmetric elements are used, which is an extension of previous work with SLA where normally only plane stress elements are used (Rots et al. 2008, DeJong et al. 2008, Invernizzi et al. 2010).

The next Section will illustrate features of the adopted bond-slip model. This bond model will be utilized in Section 6 to investigate the influence of the various material parameters. In the following Section a generic saw-tooth approximation will be presented for bond-slip. Section 4 will show the derivation of the constitutive relation for axisymmetric elements for use with SLA. Next, in Section 5 a base comparison is made between conventional NLFEA and SLA for modelling a straightforward tension-pull experiment. Finally in Section 6 several variations in reinforcement ratio and concrete type are explored in conjunction with the bond model described in Section 2.

2 BOND-SLIP MODEL

The bond-slip relation is calculated with Matlab using an adapted bond model by Bigaj (1999). The model is based upon the stress state of a thick-walled cylinder representing the concrete surrounding a single rebar. The thick-walled cylinder has a radius equal to the effective cover, see Figure 1 (right).

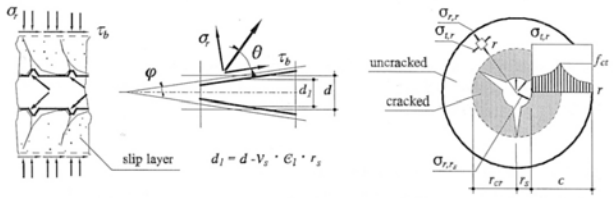

Figure 1 Definition of slip layer (left), assumption of conical interface and friction (middle) and concrete response to radial displacement of interface (right)

If a bar is pulled relative to the concrete the rebar ribs will be pushed against the concrete see Figure 1 (left). In the model this wedging effect is taken into account by conceiving the interface between the boundary layer and the surrounding concrete as conical (instead of discrete ribs), see Figure 1 (middle). In the following subsections some dependencies of the different model parameters will be presented, which will demonstrate the workings of the adapted bond model in the case of either splitting or pull-out failure. The bond model will automatically distinguish between pull-out failure and splitting failure depending on a prescribed value for the critical shear stress. In the next section the proposed saw-tooth approximation for bond-slip will be presented.

2.1 *Splitting failure*

In case of splitting failure the following dependencies are incorporated (Figures 2-4):

- increasing the effective concrete cover will increase the maximum bond stress;
- increasing the concrete strength will increase the maximum bond stress but also results in a more brittle bond behaviour;
- increasing the rebar diameter has a reverse effect on the bond-slip relation (note that the d_s-axis in Figure 4 is reversed).

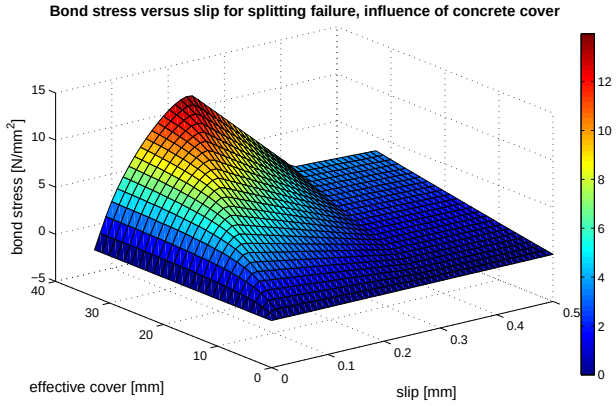

Figure 2 Bond-slip versus effective cover (d_s=12 mm, f_{cc}=35 N/mm^2, f_{ct}=2.80 N/mm^2)

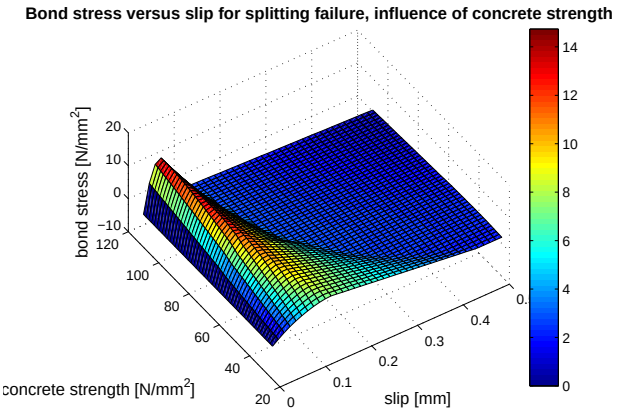

Figure 3 Bond-slip versus concrete strength (d_s=12 mm, c=20 mm)

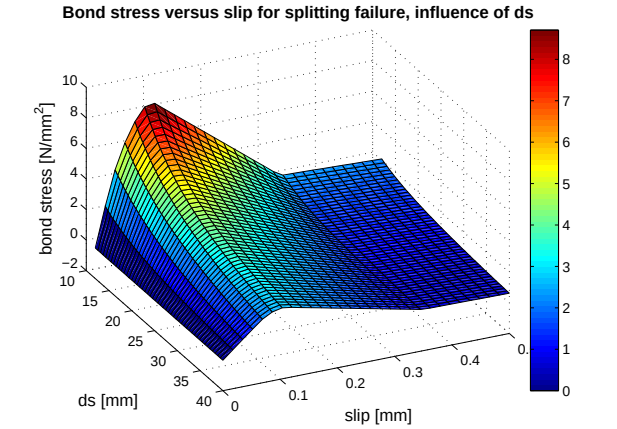

Figure 4 Bond-slip versus rebar diameter (c=20 mm, f_{cc}=35 N/mm^2, f_{ct}=2.80 N/mm^2)

2.2 *Pull-out failure*

Generally speaking, when the effective concrete cover is sufficiently increased pull-out will always be the governing failure mode. In case of pull-out failure the following dependencies are incorporated (Figures 5-7):

- increasing the longitudinal steel strain will cause the rebar to detach from the surrounding concrete resulting in decreased bond stresses;
- increasing the concrete compressive strength (and indirectly the concrete tensile strength and Young's modulus) will increase the maximum bond stress (note that the jump at a concrete strength of 62.5 N/mm^2 is caused by a difference in the calculation of the concrete tensile strength between normal strength (NSC) and high strength concrete (HSC));
- increasing the rebar diameter has a reverse effect on the bond-slip relation (the concrete cover is kept equal to 4 times the rebar diameter to prevent splitting failure).

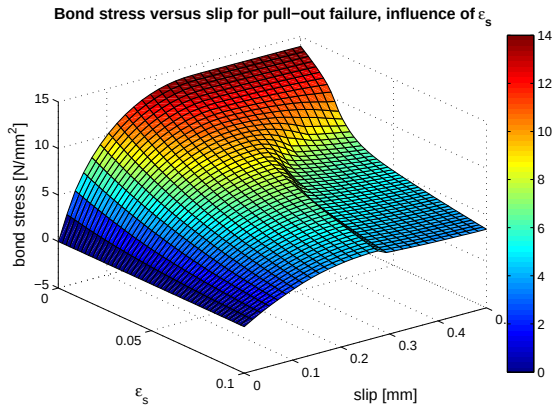

Figure 5 Bond-slip versus steel strain ε_s (d_s=12 mm, c=40 mm, f_{cc}=35 N/mm^2, f_{ct}=2.80 N/mm^2)

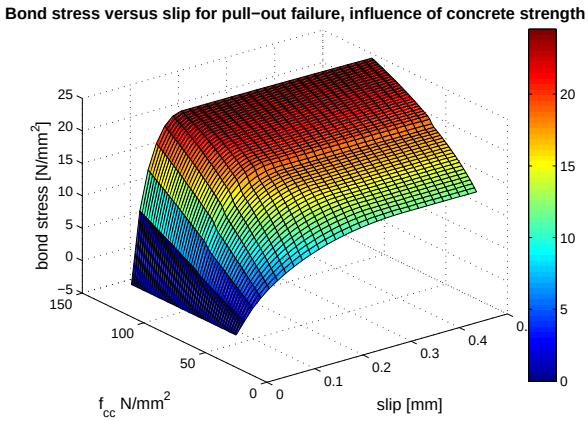

Figure 6 Bond-slip versus concrete strength (d_s=12 mm, c=40 mm, ε_s=0)

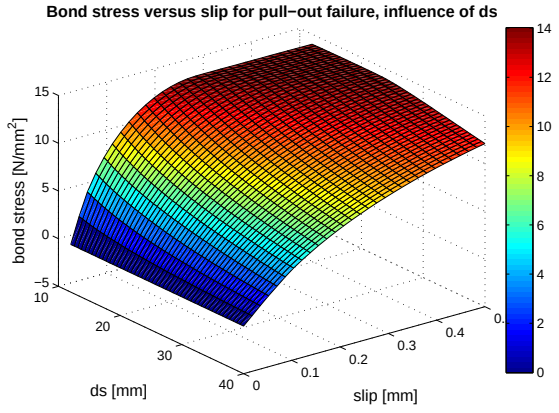

Figure 7 Bond-slip versus d_s (c=4d_s mm, ε_s=0, f_{cc}=35 N/mm^2, f_{ct}=2.80 N/mm^2)

3 SAW-TOOTH MODELING OF BOND

Sequentially Linear Analysis requires saw-tooth approximations of the material models. It comes down to assuming a piecewise linear material behaviour,

separated by damage increments. The smaller the damage increments, the closer the approximation.

Figure 8 gives an example of a saw-tooth approximation for concrete in tension.

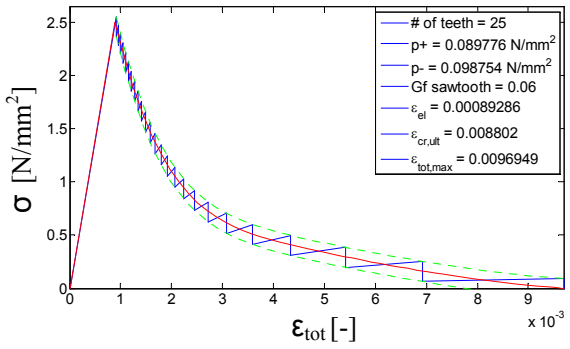

Figure 8 Example of a saw-tooth approximation for nonlinear concrete softening

In this example 25 teeth are used to approximate the original nonlinear curve representing the concrete softening. For concrete softening the area underneath the softening curve represents the fracture energy. This must be equal to the area underneath the saw-tooth approximation (Rots et al. 2008).

Since bond-slip curves are already nonlinear for low values of slip only a limited elastic part is assumed. Therefore the saw-tooth approximation will start already on the ascending part of the curve. In general terms a damage increment in SLA applies to the stiffness only, which is reduced in each increment as the strength can either be increased or decreased depending on the type of material at hand. For bond-slip an equal and constant uplifting and downshifting of the mother curve is assumed (expressed as p^+; p^-). The nonlinear bond-slip curve can be imitated by consecutively reducing the stiffness as well as either reducing or increasing the bond strength. The Equations 1-4 provide the first part of the saw-tooth approximation for bond stress (τ), slip (δ) and stiffness (G):

$$\tau_1^+ = \tau_{el;\max} + p^+ \quad (1)$$

$$\tau_1^- = \tau_1^+ - 2p^+ \quad (2)$$

$$\delta_1 = \frac{\tau_1^+}{G_{el}} \quad (3)$$

$$G_1 = \frac{\tau_1^-}{\delta_1} \quad (4)$$

where G_1 represents the first reduced stiffness. The subsequent values for τ_{i+1}^+ and δ_{i+1} can be found numerically, if necessary, as the intersection of the reduced stiffness and the uplifted curve. These values in turn provide the subsequent values for the reduced stiffness:

$$G_{i+1} = \frac{\tau_{i+1}^+ - 2p^+}{\delta_{i+1}} \quad (5)$$

The procedure can be applied to any shape of the bond-slip curve. The number of teeth (N) combined with the offset value (p^+;p^-) can be chosen dependent on the desired accuracy and the maximum slip expected to occur in the present calculation. Figure 9 shows the results of applying the proposed procedure in the case of a simple bi-linear bond-slip curve.

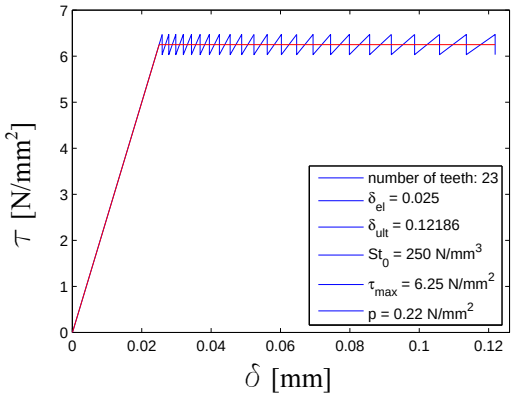

Figure 9 Sawtooth approximation for bi-linear bond-slip

Figures 10-11 show examples of saw-tooth approximations for bond-slip in case of splitting and pull-out failure where the "mother" curve has been calculated using the adapted bond model described in Section 2. Note that bond-slip is not dependent on slip direction; therefore the same saw-tooth is valid for negative as well as positive slip values.

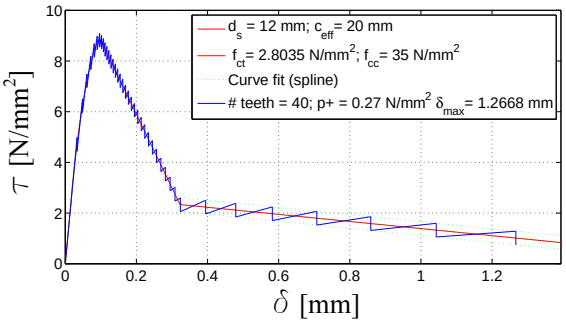

Figure 10 Numerical sawtooth approximation for splitting failure

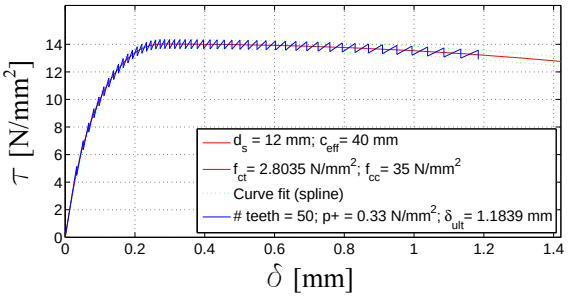

Figure 11 Numerical sawtooth approximation for pull-out failure

4 AXISYMMETRIC ELEMENTS IN SLA

For axisymmetric elements the derivation of the constitutive relation is an extension of previous work where normally plane stress elements are used. The stress-strain relation is based upon (reduced) Young's modulus in the orthogonal (crack) directions: *n*, *t* and *z*. The *z*-direction represents the added circumferential direction. In this local crack axes system the relation between the stresses and the strains for an axisymmetric element is given by:

$$\begin{bmatrix} \sigma_{nn} \\ \sigma_{tt} \\ \sigma_{zz} \\ \sigma_{nt} \end{bmatrix} = \mathbf{D} \begin{bmatrix} \varepsilon_{nn} \\ \varepsilon_{tt} \\ \varepsilon_{zz} \\ \gamma_{nt} \end{bmatrix} \tag{6}$$

with **D** denoted as

$$F \begin{bmatrix} (\upsilon_{tz}\upsilon_{zt}-1)E_n & -(\nu_{nz}\nu_{zt}+\nu_{nt})E_n & -(\nu_{nt}\nu_{tz}+\nu_{nz})E_n & 0 \\ -(\nu_{zn}\nu_{tz}+\nu_{tn})E_t & (\nu_{zn}\nu_{nz}-1)E_t & -(\nu_{tn}\nu_{nz}+\nu_{tz})E_t & 0 \\ -(\nu_{tn}\nu_{zt}+\nu_{zn})E_z & -(\nu_{zn}\nu_{nt}+\nu_{zt})E_z & (\nu_{tn}\nu_{nt}-1)E_z & 0 \\ 0 & 0 & 0 & \frac{G}{F} \end{bmatrix} \tag{7}$$

in which E_n, E_t and E_z are the reduced (or damaged) Young's' moduli in the three orthogonal directions. The shear modulus G is derived from the initial shear modulus G_0

$$G_0 = \frac{E_0}{2(1+\nu_0)} \tag{8}$$

based on a shear retention model by DeJong et. al (2008). F equals

$$F = \frac{1}{(\nu_{zn}\nu_{nt}\nu_{tz}+\nu_{tn}\nu_{nz}\nu_{zt}+\nu_{zn}\nu_{nz}+\nu_{tn}\nu_{nt}+\nu_{tz}\nu_{zt}-1)} \tag{9}$$

Where the Poisson's ratios are determined as

$$\nu_{ij} = \nu_0 \left(\frac{E_j}{E_0} \right) \tag{10}$$

Here the subscript *j* indicates the source stress direction. Now Equation 10 yields three unique values, which in turn result in a fully symmetrical constitutive matrix in Equation 7.

5 TENSION-PULL EXPERIMENT (1)

In this section results will be presented of a FEM calculation of a tension-pull experiment by Gijsbers (1977). A comparison between conventional NLFEA and SLA will show promising results for SLA modelling regarding the use of axisymmetric and interface elements. In this section a simple elastoplastic model is assumed for bond-slip according to Figure 9.

5.1 *FE modelling aspects*

The tension-pull experiment consists of a single reinforcing bar with a square concrete cover, see Figure 12. For the FEM discretization the square concrete cover is replaced by an equivalent circular cover.

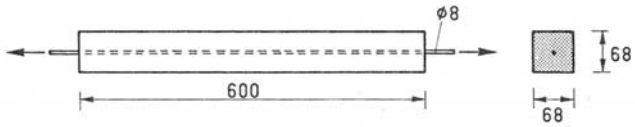

Figure 12 Tension-pull experiment by Gijsbers (1977)

The mesh, consisting of axisymmetric elements for the concrete, truss elements for the reinforcing bar and interface elements for bond-slip, is given in Figure 13. The loading consists of a displacement u_y at the right end, whereas the left end is fixed.

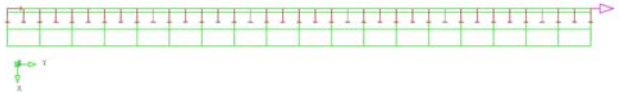

Figure 13 Finite element mesh of tension-pull experiment, boundary conditions and loading

The material models used comprise of nonlinear Hordijk tension softening for the concrete (tensile strength f_{ct} = 2.5 N/mm^2, Young's modulus E=28000

N/mm^2, fracture energy G_f=0.06 N/mm and crack band width h=11.11 mm), elastoplastic bond-slip (ultimate tangential bond stress τ_u = 6.25 N/mm^2, tangential stiffness S_t=250 N/mm^3 and normal stiffness S_n = 20000 N/mm^3) and elastoplastic steel (yield stress σ_y = 400 N/mm^2 and Young's modulus E=192300 N/mm^2).

The original load-displacement curve of the experiment is given in figure 14.

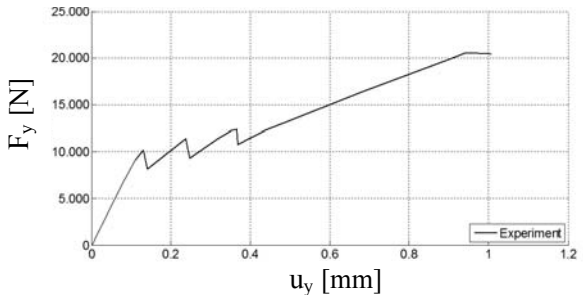

Figure 14 Load-displacement curve Gijsbers

5.2 *NLFEA versus SLA*

To simulate the experiment and to compare results between NLFEA and SLA it is necessary to include material imperfections. Without imperfections the NLFEA will not show any crack localization. Material imperfections can be incorporated in various ways. Often a reduction of the concrete tensile strength is used. However if the fracture energy and the crack band width remain unchanged this will also result in an increase of the ultimate crack strain. The method of creating an imperfection however is somewhat arbitrary. It is therefore proposed to reduce the fracture energy by a quadratic reduction factor and the tensile strength by a constant reduction factor. This will result in an equal reduction of the ultimate crack strain and the tensile strength, see figure 15.

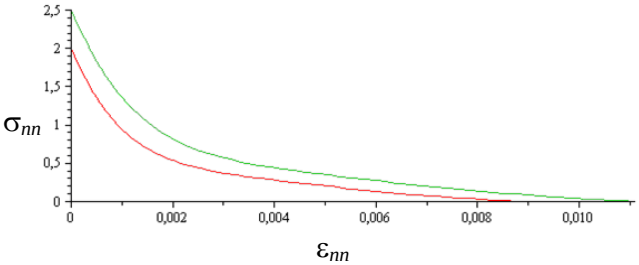

Figure 15 Effect of combined reduction of tensile strength and ultimate crack strain with Hordijk softening (reduction factor 0.8)

The material imperfections, using different reduction factors, are applied to cross-sections at ¼ *L*, ½ *L* and ¾ *L* of the length *L* of the tie. Figure 16 shows the results for the NLFEA and the SLA calculation in a load-displacement curve.

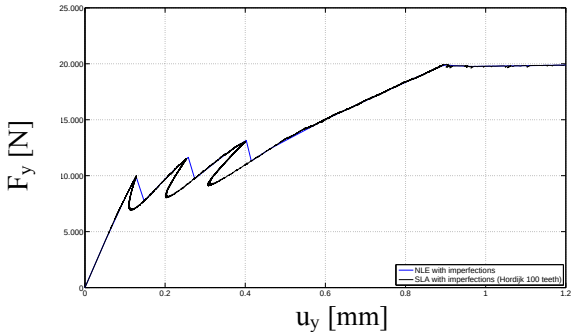

Figure 16 Load-displacement curve NLFEA versus SLA

The results show that the NLFEA and SLA are in agreement. From Figure 16 it becomes clear that distinct snapbacks are captured when using SLA which is in accordance with previous work (Invernizzi et al. 2011, Rots et al. 2011). For the analysis the simulation of these snapbacks is important, as it indicates the energy release caused by each crack, by following the quasi-static equilibrium path. Other results also show great similarity between NLFEA and SLA demonstrating the correct workings of the adopted axisymmetric and interface elements in SLA. Figure 17 shows the crack strains at various load levels when using SLA whereas Figures 18-19 show the bond stress profiles along the interface.

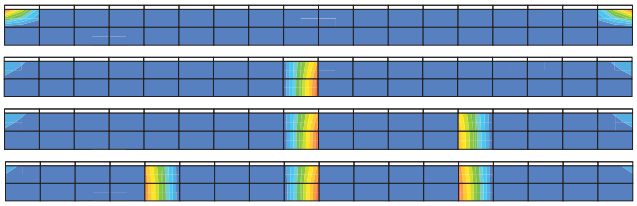

Figure 17 Crack strain ε_{cr}^{nn} at u$_y$=0.1 mm, u$_y$=0.2 mm, u$_y$=0.3 mm and u$_y$=0.6 mm

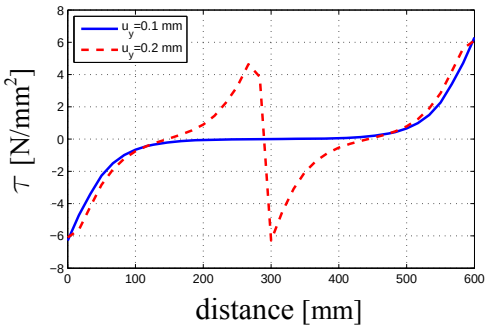

Figure 18 Bond stress profiles (u_y = 0.1 mm, u_y=0.2 mm)

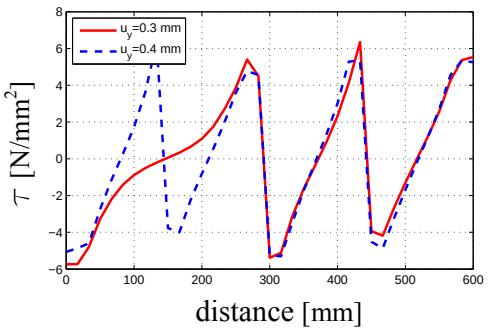

Figure 19 Bond stress profiles (u_y=0.3 mm, u_y=0.4 mm)

The three primary cracks represent a fully developed crack pattern. Since forces are transferred to the surrounding concrete by bond the crack spacing makes it impossible for new cracks to develop. The ultimate load level is finally governed by yielding of the rebar.

5.3 *SLA without material imperfections*

In the previous subsection a comparison between NLFEA and SLA showed promising results when using material imperfections. However since SLA is governed by damage increments there is no need to impose material imperfections. Therefore the same analyses can be carried out using SLA without material imperfections. Figure 20 shows the results in a load-displacement curve together with the previously obtained NLFEA curve. The crack strains at various load levels are shown in Figure 21. Despite the initial nearly uniform stress distribution the results show sharp crack localizations.

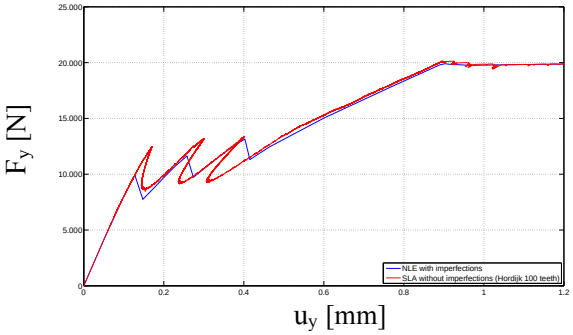

Figure 20 Load-displacement curve NLFEA using imperfections versus SLA without imperfections

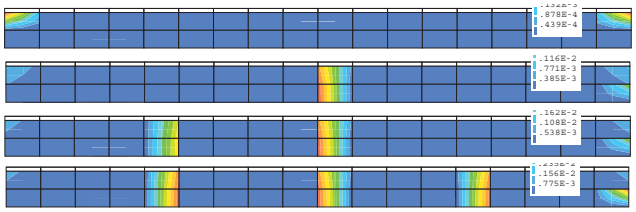

Figure 21 Crack strain ε_{cr}^{nn} at u_y=0.1 mm, u_y=0.2 mm, u_y=0.3 mm and u_y=0.6 mm

6 TENSION-PULL EXPERIMENT (2)

In this section several large scale tension-pull experiments by Mayer (2001) will be simulated using SLA and the adapted bond model (see Section 2). Variations in concrete type and reinforcement ratio are applied to demonstrate their respective influence on the crack spacing.

6.1 *FE modelling aspects*

The tension-pull experiments consist of long specimens (2.3 to 2.9 m) and have a square concrete cross-section (300×300 mm or 400×400 mm) with rebars located in the corners and/or near the sides, see Figure 17 (left). The proposed discretization is given in Figures 22-23. In figure 22 the square reinforced concrete section is transformed into an equivalent circular section and the rebar cross-sections are lumped together to a position with equal concrete cover. Since the reinforcement is not part of the axi-symmetry this is equivalent to Figure 22 middle.

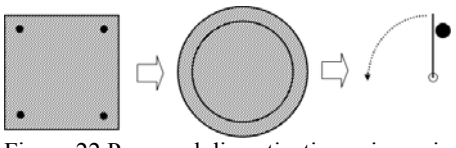

Figure 22 Proposed discretization using axi-symmetry and lumped rebars

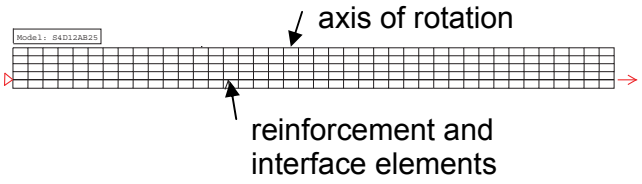

Figure 23 Mesh for dimensions 300x300x2500 mm

6.2 *Influence of reinforcement ratio*

Figure 24 demonstrates the influence of reinforcement ratio on the fully developed crack pattern. From a modelling perspective only the circumference for the interface elements and the truss cross section, representing the lumped rebars, differs. In both cases the same bond-slip relation is valid and therefore the same saw-tooth approximation is being used. Especially for 8Ø12, the crack evolution is noteworthy. The first crack starts at midpoint followed by subsequent divisions in crack spacing until the final crack pattern emerges.

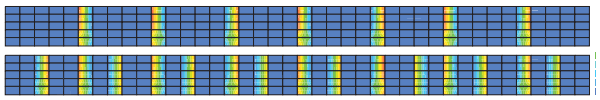
Figure 24 Final crack pattern, 4 bars Ø12 (top) versus 8 bars Ø 12 (bottom)

6.3 *Influence of concrete type*

Figure 25 demonstrates the influence of concrete type (B25 versus B45) on the fully developed crack pattern. In both cases the reinforcement consists of 8Ø12. The bond-slip relation in both simulations differs (see also Figure 6). Compared to B25 the increased bond-slip stiffness for B45 causes a quicker load transfer from the rebar into the surrounding concrete resulting in a denser crack spacing (132 mm for B45 versus 156 mm for B25).

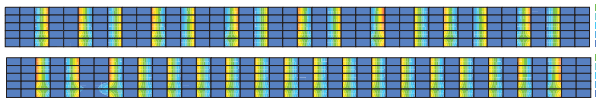
Figure 25 Final crack pattern, 8Ø12 B25 (top) versus B45 (bottom)

7 CONCLUSIONS

A sequentially linear approach has been proposed for bond-slip using concrete-to-steel interface elements. A generic procedure for a saw-tooth approximation applicable to any shape of the bond-slip curve has been proposed. A direct comparison between NLFEA and SLA has validated the use of SLA for interface and axisymmetric elements. Despite the highly uniform stress distribution inherent to the analysis of a tension-pull experiment it has been proven that SLA does not require material imperfections to obtain stable crack localizations. The use of an advanced bond model has demonstrated the ability to obtain crack spacings with characteristics equal to real life experiments.

REFERENCES

Bigaj, A.J. 1999. Structural Dependence of Rotation Capacity of Plastic Hinges in RC Beams and Slabs. Ph.D Dissertation. Delft University of Technology 2000.

DeJong, M.J., Hendriks, M.A.N., Rots, J.G. 2008. Shear retension and mesh alignement during fracture using sequentially linear analysis. In “12th International Conference on Fracture”, 12-17 July 2009, Ottawa, Canada

Ensink, S.W.H. 2010. Simulation of steel-concrete bond-slip with sequentially linear analysis using interface elements. Msc Thesis Faculty of Civil Engineering and Geosciences Delft University of Technology.

Gijsbers, F.B.J., Hehemann, A.A. 1977. Some tensile tests on reinforced concrete. TNO-IBBC Report BI-77-61, Rijswijk.

Invernizzi, S., Trovato, D., Hendriks, M.A.N., van de Graaf, A.V. 2011. “Sequentially linear modelling of local snap-back in extremely brittle structures”, Engineering Structures, 33, 1617-1625.

Mayer, U. 2001. Influence of the rib pattern of ribbed reinforcement on the structural behavior of reinforced concrete members. Ph.D Dissertation. University of Stuttgart.

Rots, J.G., Belletti, S., Invernizzi, S. 2008. Robust modeling of RC structures with an "event-by-event" strategy. Engineering Fracture Mechanics 75, 590-614.

Rots, J.G., Hendriks, M.A.N. 2011. Sequentially linear versus nonlinear analysis of RC structures. In "International conference on recent advances in nonlinear models - Structural concrete applications", CoRAN 2011.